The Journal of Neuroscience, March 15, 1996, 16(6):1990–2001

G-Protein-Gated Inward Rectifier K^+ Channel Proteins (GIRK1) Are Present in the Soma and Dendrites as well as in Nerve Terminals of Specific Neurons in the Brain

Arturo Ponce,[1] Earl Bueno,[1] Clifford Kentros, [1] Eleazar Vega-Saenz de Miera,[1] Alan Chow,[1] Dean Hillman,[1] Susan Chen, [1] Liangxue Zhu,[2] Michael B. Wu,[2] Xiaying Wu,[2] Bernardo Rudy,[1] and William B. Thornhill[2]

[1]Department of Physiology and Neuroscience, New York University Medical Center, New York, New York 10016, and [2]Department of Physiology and Biophysics, Mount Sinai School of Medicine, New York, New York 10029

G-protein-gated inward rectifier potassium (GIRK) channels are coupled to numerous neurotransmitter receptors in the brain and can play important roles in modulating neuronal function, depending on their localization in a given neuron. Site-directed antibodies to the extreme C terminus of GIRK1 (or KGA1), a recently cloned component of GIRK channels, have been used to determine the relative expression levels and distribution of the protein in different regions of the rat brain by immunoblot and immunohistochemical techniques. We report that the GIRK1 protein is expressed prominently in the olfactory bulb, hippocampus, dentate gyrus, neocortex, thalamus, cerebellar cortex, and several brain stem nuclei. In addition to the expected localization in somas and dendrites, where GIRK channels may mediate postsynaptic inhibition, GIRK1 proteins were also found in axons and their terminal fields, suggesting that GIRK channels can also modulate presynaptic events. Furthermore, the distribution of the protein to either somatodendritic or axonal-terminal regions of neurons varied in different brain regions, which would imply distinct functions of these channels in different neuronal populations. Particularly prominent staining of the cortical barrels of layer IV of the neocortex, and the absence of this staining with unilateral kainate lesions of the thalamus, suggest that the GIRK1 protein is expressed in thalamocortical nerve terminals in which GIRK channels may mediate the actions of μ opiate receptors.

Key words: thalamocortical projections; opiate receptors; immunocytochemistry; antibodies; dendritic channels; presynaptic modulation

Neurons express various voltage-, ligand-, and second messenger-gated ion channels that are responsible for the electrical excitability of the cell, its characteristic action-potential duration and waveform, its response to incoming signals, and the release of neurotransmitter at its nerve terminal (Hille, 1992). G-protein-gated inward rectifier potassium channels (GIRKs) from atrial myocytes are activated by pertussis toxin-sensitive heterotrimeric G-proteins in a membrane-delimited pathway (Brown and Birnbaumer, 1990; Hille, 1992), and both the Gα-GTP subunit (Codina et al., 1987; Yatani et al., 1988) and the G$\beta\gamma$ subunit (Logothetis et al., 1987; Wickman et al., 1994) have been proposed to be the major activator of the channel. These channels are important mediators of neurotransmitter actions in the heart and the brain (Brown and Birnbaumer, 1990; Hille, 1992). For example, in the heart, acetylcholine (ACh) released from the vagus nerve binds to atrial m2 muscarinic receptors. ACh-binding to the receptor results in the release of G-protein subunits that activate a GIRK channel known as IKACh, resulting in the slowing of the heart rate (Breitwieser and Szabo, 1985; Pfaffinger et al., 1985; Hille, 1992). In neurons, GIRK channels have been found to be coupled to numerous neurotransmitter receptors such as m2 muscarinic, μ and δ opioid, 5-HT1A serotonin, histamine, A1 adenosine, D2 dopamine, somatostatin, α2-adrenergic, γ-aminobutyric acid type B, and galanin receptors. These channels play an important role in modulating neuronal activity by generating inhibitory postsynaptic potentials, thereby inhibiting action-potential generation in postsynaptic neurons (North, 1989; Brown and Birnbaumer, 1990).

Recently, molecular components of a GIRK channel termed GIRK1, KGA1, or Kir3.1 have been cloned from rat atria and brain and expressed functionally in *Xenopus* oocytes (Dascal et al., 1993; Kubo et al., 1993). The G$\beta\gamma$ subunit seems to be the major activator of this channel (Reuveny et al., 1994). On the basis of the deduced amino acid sequence, we have raised antibodies specific for the GIRK1 protein and have used these antibodies to determine the relative expression levels and the localization of the protein in different regions of the rat brain by immunoblotting and immunohistochemical techniques. We report that the GIRK1 protein is localized in different areas of the brain to either somatodendritic or axonal-terminal regions of neurons in which activation of this channel would be predicted to have different modulatory effects on neuronal excitability.

MATERIALS AND METHODS

GIRK1 cDNA probes. GIRK1 was cloned from an atrial cDNA library using a cDNA probe to the M1-H5-M2 domain that was generated by reverse transcriptase-PCR from atrial RNA (Kubo et al., 1993). Positive clones were subcloned into pBluescript (Stratagene, La Jolla, CA), and both cDNA strands were sequenced by standard methods (Ausubel et al., 1990). cDNA probes for *in situ* hybridization histochemistry to the 5′ end [base pair (bp) 1–249, encoding amino acids 1–83 at the N terminus] or the 3′ end (bp 1071–1503, encoding amino acids 357–501 at the C terminus) of GIRK1 were generated by PCR and subcloned

Received Aug. 22, 1995; revised Dec. 18, 1995; accepted Dec. 19, 1995.

This research was supported by National Institutes of Health Grant NS29633 to W.B.T., and National Institutes of Health Grant NS30989 and National Science Foundation Grant IBN 9209523 to B.R. A.P. is a fellow of the Human Frontiers Science Program.

Correspondence should be addressed to Dr. William B. Thornhill, Department of Physiology and Biophysics, 1 Gustave Levy Place, Mount Sinai School of Medicine, New York, NY 10029.

into pBluescript. The isolated cDNA inserts were labeled with ^{32}P-deoxycytidine 5′-triphosphate (dCTP) by random priming (Ausubel et al., 1990).

Northern blot analysis. PolyA mRNAs (3 μg/lane) were run on a 1% agarose gel, transferred to a nylon membrane, and hybridized with a radiolabeled probe to the untranslated 3′ end of GIRK1. The probe was labeled with ^{32}P-dCTP by the PCR method (Ausubel et al., 1990). The filters were incubated in prehybridization solution for 1 hr and hybridized at high stringency [50% formamide/42°C/2× SSPE (0.15 M NaCl, 1 mM EDTA, 10 mM NaH_2PO_4, ph 7.4)] with the probe for 15 hr. The filters were then washed, and the final high stringency wash was in 0.2× SSPE at 60°C. The blot was exposed to the film for 20 hr.

Production of antibody. A peptide (CGPTRMEGNLPAKLRKMNSDRFT) to the extreme C terminus of GIRK1 (480–501) was synthesized and purified, and its amino acid composition was verified by standard methods by Dr. A. Buku in the Department of Physiology and Biophysics, Mount Sinai Medical Center. The peptide was coupled through a terminally added cysteine residue to keyhole limpet hemocyanin (KLH). The peptide-KLH conjugate was injected into rabbits, and the antiserum was collected for characterization. The GIRK1 peptide was covalently attached to Sulfo-link Sepharose beads (Pierce, Rockford, IL), and the antiserum was affinity-purified following the protocols of the vendor. Only affinity-purified antibodies were used in this study.

Transfection of Chinese hamster ovary (CHO) cells with cDNA for GIRK1. A GIRK1 cDNA encoding a complete open reading frame was subcloned into pcDNA3 (Invitrogen, San Diego, CA), and CHO cells were transfected by the calcium phosphate method (Ausubel et al., 1990). Neomycin-resistant clones were picked for further analysis by immunoblotting using the GIRK1 antibody.

Preparation of membranes. Adult Sprague–Dawley rat brain membrane extracts were prepared from a P3 fraction of tissue homogenate (Hartshorne and Catterall, 1984) solubilized for 1 hr in a 2% Triton X-100 solution containing 50 mM potassium phosphate buffer, pH 7.4, 50 mM KCl, and 2 mM EDTA, and 1 mM pepstatin A, 1 mM 1,10 phenanthroline, 0.2 mM phenylmethylsulfonyl fluoride, and 1 mM iodoacetamide to inhibit proteases. The suspension was spun at 100,000 × *g* to remove nonsolubilized material, and the top two thirds of the supernatant was used for further experiments. Membranes from confluent CHO cell cultures were prepared by homogenizing the cells in a 25 mM potassium phosphate, pH 7.4, 2 mM EDTA ice-cold solution containing the aforementioned protease inhibitors. Membranes were pelleted at 35,000 × *g* for 1 hr, resuspended in the same solution at 2–3 mg/ml, and stored at −70°C. Before use, the membranes were thawed and solubilized as above.

Immunoblot analysis. Seventy-five micrograms of membrane protein from different regions of the rat brain were denatured in SDS sample buffer, SDS-PAGE electrophoresis was performed, and the proteins were electrotransferred to nitrocellulose membranes for immunoblotting (Harlow and Lane, 1988). The filter was incubated in GIRK1-antibody at a 1:2000 dilution. The specific proteins were detected by incubation in secondary antibody (donkey anti-rabbit horseradish-peroxidase conjugate) followed by chemiluminscence with a chemiluminescence kit (Amersham, Buckinghamshire, UK).

In situ *hybridization and immunocytochemistry.* Adult male Sprague–Dawley rats were anesthetized with sodium pentobarbital (Nembutal, 120 mg/kg, i.p.) and perfused transcardially with cold saline containing 0.5% $NaNO_2$ and 10 U/ml heparin followed by 400 ml of cold 0.1 M phosphate buffer containing 4% formaldehyde. The brains were removed, cut into appropriate blocks, and postfixed for 2 hr, after which they were placed in 30% sucrose at 4°C overnight. Tissue sections (30–40 μm, unless otherwise indicated) were cut on a freezing sliding microtome and processed for *in situ* hybridization histochemistry or immunohistochemistry. *In situ* hybridization of floating sections used protocols described previously (Rudy et al., 1992; Weiser et al., 1994). For immunocytochemistry, the brain sections (Moreno et al., 1995; Weiser et al., 1995) were preincubated for 60 min in a blocking solution of 0.1 M PBS with 2% bovine serum albumin (Sigma Fraction V; Sigma, St. Louis, MO), 0.1% Triton X-100, 20 μl/ml goat serum, 100 μl/ml fetal bovine serum, 10 μl/ml biotin, and 0.1 μl/ml H_2O_2. The sections were then washed in PBS containing 0.1% Triton X-100 (PBST) and incubated overnight with anti-GIRK1 antibodies (1:100, unless otherwise indicated) in blocking solution without biotin and H_2O_2. After washing in PBST, the sections were incubated for 1 hr with biotinylated anti-rabbit IgG (1:200) (Vector Laboratories, Burlingame, CA). The tissue was rinsed and incubated for 1 hr with the avidin-biotin-horseradish peroxidase complex according to Vectastain Elite ABC kit instructions (Vector Laboratories). The antigen-antibody complexes were visualized by reaction with the chromogen 3,3′-diaminobenzidine-tetrahydrochloride (DAB) (Aldrich, Milwaukee, WI) and H_2O_2 for 5 min or (see Fig. 8*B,C,F*) by a 1–2 min reaction with DAB with nickel amplification, as described by the supplier (Pierce, Rockford, IL). Sections were mounted on slides and processed as described in Weiser et al. (1995).

Kainic acid lesions of the thalamus were performed as described previously (Moreno et al., 1995). Briefly, adult male rats (275–300 gm) were anesthetized deeply with an intraperitoneal injection of 100 mg/kg ketamine and 10 mg/kg xylazine and placed in a stereotaxic apparatus. When a small piece of the overlying skull was removed, 100 nl of 10 mg/ml kainic acid was injected with a glass micropipette into the ventromedial/ventroposterior thalamic area [AP +6.7 mm, ML +1.2 mm, DV +6.8 mm; according to the atlas of Paxinos and Watson (1986)] for a period of 10 min using a Drummond 10 μl microdispenser. The micropipette was kept in place an additional 10 min to minimize diffusion of the neurotoxin into the injection shaft, after which the wound was packed with Gelfoam and sutured, and the animals were allowed to recover from the anesthetic.

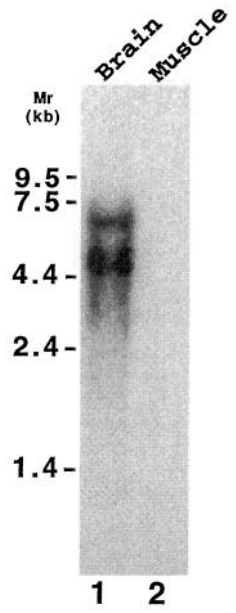

Figure 1. Northern blot analysis of GIRK1 mRNA. A 3′ untranslated ^{32}P-radiolabeled cDNA probe to GIRK1 was used for Northern blot analysis of polyA mRNA (3 μg) from rat brain and skeletal muscle. The film was exposed to the nylon membrane for 20 hr. The positions of RNA markers (in kilobases) are shown on the *left* of the blot.

RESULTS

Northern blot analysis of GIRK1 mRNA

Northern blot analysis of rat brain mRNA with a radiolabeled probe to the 3′ untranslated region of GIRK1 revealed two distinct bands between 7.5 and 4.4 kb, whereas no signal was detected in skeletal muscle (Fig. 1, *lanes 1* and *2*, respectively), as has been reported previously (Dascal et al., 1993; Kubo et al., 1993).

Localization of GIRK1 mRNA in rat brain by *in situ* hybridization

Our results of mRNA localization by *in situ* hybridization resembled those of Karschin et al. (1994). In the rat brain, GIRK1 hybridization signals were strongest in the olfactory bulb, hippocampus, and dentate gyrus (Fig. 2). Strong signals were also

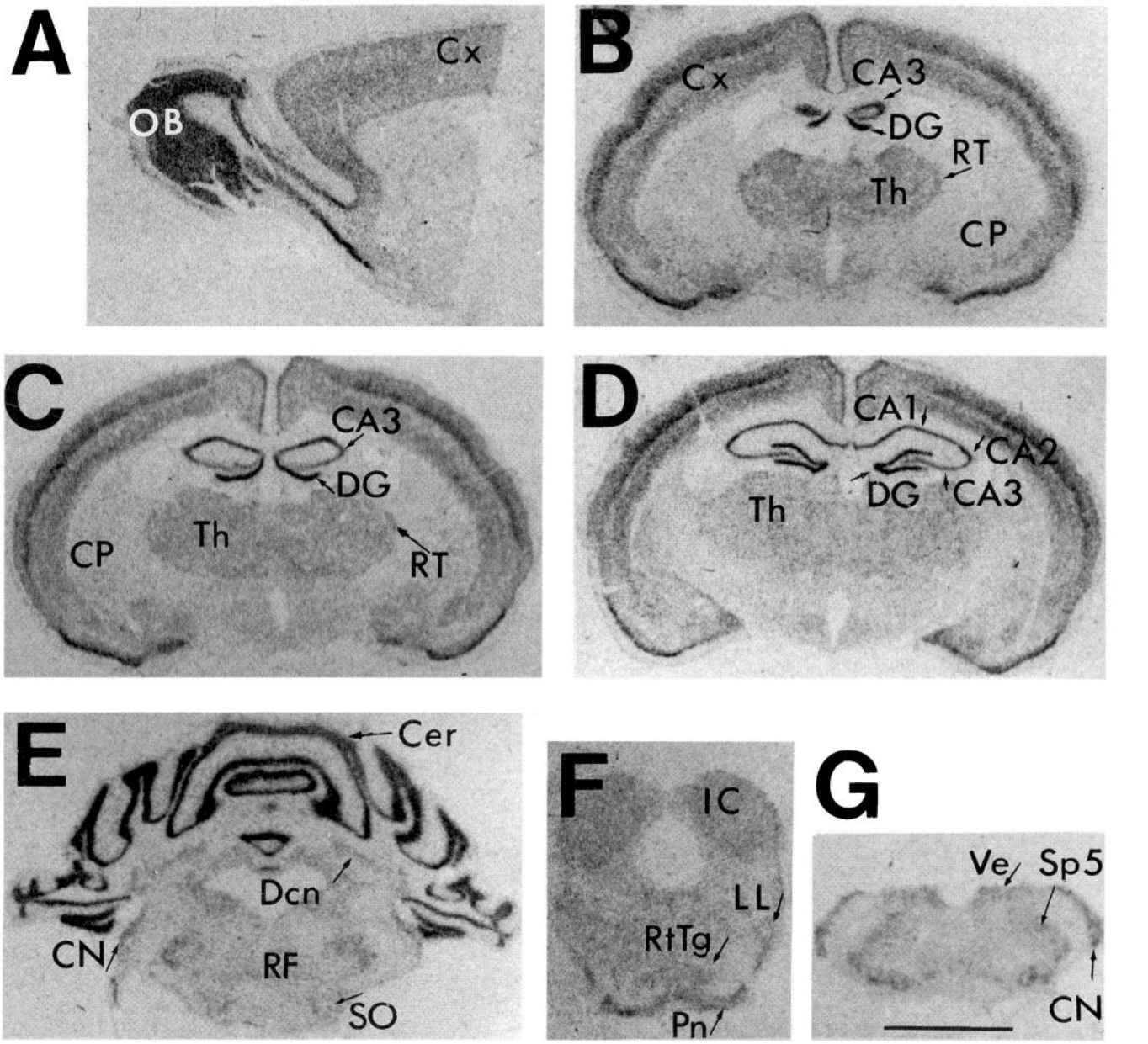

Figure 2. Localization of GIRK1 mRNAs in the rat brain. Photomicrographs of the autoradiograms of rat brain sections after *in situ* hybridization histochemistry with the 3′ cDNA probe. Identical results were obtained with the 5′ probe (data not shown). *A*, Sagittal section through the olfactory bulb, illustrating strong labeling of the main olfactory bulb and the anterior olfactory nuclei. *B*, Coronal section of the forebrain at the level of the anterior portion of the hippocampus. *C*, Coronal section of the forebrain posterior to the section shown in *B*. *D*, Coronal section of the forebrain posterior to the section shown in *C*. *E*, Coronal section at the level of the cerebellum. *F*, Coronal section at the level of the inferior colliculus (without the overlying cortex). *G*, Coronal section at the level of the medulla. Note the specific regional expression of the GIRK1 mRNA (*dark areas*) and the lack of significant staining in the caudate–putamen (*B*, *C*). Abbreviations: *CA1*, CA1 region of the hippocampus; *CA2*, CA2 region of the hippocampus; *CA3*, CA3 region of the hippocampus; *Cer*, cerebellar cortex; *CN*, cochlear nuclei (ventral in *E* and dorsal in *G*); *CP*, caudate–putamen; *Cx*, neocortex; *Dcn*, deep cerebellar nuclei; *DG*, dentate gyrus; *IC*, inferior colliculus; *LL*, lateral lemiscus nuclei; *OB*, olfactory bulb; *Pn*, pontine nucleus; *RF*, reticular formation; *RT*, reticular thalamic nucleus; *RtTg*, reticulotegmental nucleus of the pons; *SO*, superior olive; *Sp5*, spinal trigeminal nucleus; *Th*, dorsal thalamus; *Ve*, vestibular nuclei. Scale bar: 3.2 mm in *A*; 3.4 mm in *B*; 3.3 mm in *C*, *D*; 3.2 mm in *E*, *F*; 3 mm in *G*.

seen in the neocortex, the dorsal thalamus and reticular thalamic nucleus, the cerebellar cortex, and the deep cerebellar nuclei. Several nuclei in the brainstem, including the red nucleus, pontine nucleus, superior and inferior colliculi, superior olive, cochlear nuclei, reticular formation, and principal and spinal trigeminal nuclei, also displayed strong to moderate signals. Moderate to weak signals were seen in the hypothalamus. Weak to background signals were observed in the striatum, globus pallidus, and substantia nigra.

Characterization of GIRK1 antibodies and immunoblot analysis of rat brain membrane proteins

Rabbit polyclonal antibodies were raised against a synthetic peptide to the extreme C terminus of GIRK1. This peptide shares no

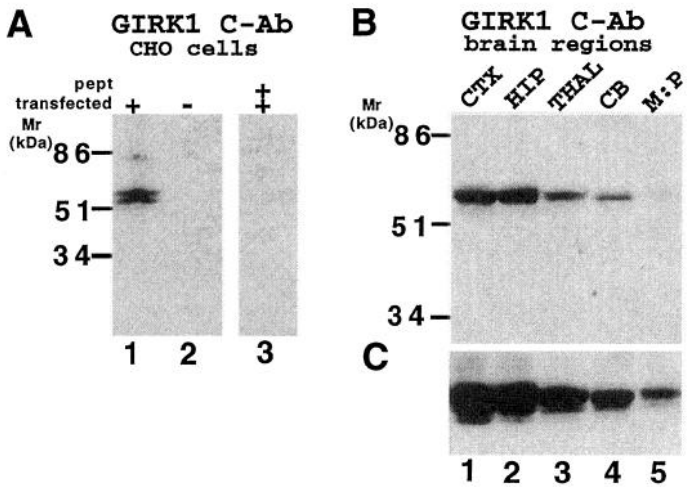

Figure 3. Immunoblot analysis of GIRK1 protein. *A*, Specificity of anti-GIRK1 antibodies (*C-Ab*). Membrane proteins from CHO cells that were stably transfected with GIRK1 cDNA and untransfected controls were run on an SDS gel for immunoblotting. The blots were incubated with the C-Ab and the GIRK1 protein detected by chemiluminescence. *Lane 1*, Membrane proteins from CHO cells transfected with GIRK1 cDNA; *lane 2*, membrane proteins from untransfected, control CHO cells; *lane 3*, separate immunoblot of membrane proteins from CHO cells transfected with GIRK1 cDNA where the C-Ab was incubated with an excess of C-terminal peptide (20 μM). *B*, *C*, Distribution of GIRK1 protein in rat brain. Rat brain membrane proteins (75 μg/lane) from different regions of the brain were run on an SDS gel for immunoblotting as in *A*. In *B*, the blot was exposed to the film for 30 sec, whereas in *C*, the same blot was exposed for 5 min. *CTX*, Cortex; *HIP*, hippocampus; *THAL*, thalamus; *CB*, cerebellum; *M:P*, medulla–pons.

identity with other recently cloned inwardly rectifying channels, including GIRK2 and GIRK3 (Lesage et al., 1994). The specificity of the affinity-purified C terminus antibody (C-Ab) was confirmed in immunoblots of membrane proteins from GIRK1 cDNA-transfected and control nontransfected CHO cells. The C-Ab recognized a protein doublet of ~54–56 kDa in membranes from GIRK1-transfected cells, whereas no immunoreactivity was seen with extracts from membranes from nontransfected control cells (Fig. 3*A*, *lanes 1* and *2*, respectively). The higher M_r band presumably represents the glycosylated GIRK1 protein. Preblocking the C-Ab with the C-terminal peptide prevented the immunoreactivity, demonstrating the specificity of the antibody reaction (Fig. 3*A*, *lane 3*). Next we determined the relative levels of GIRK1 protein expressed in five regions of the rat brain by immunoblot analysis of equal amounts of membrane proteins. The C-Ab recognized a similar protein band at an M_r of ~65 kDa from all regions of the brain tested, although at different intensities (Fig. 3*B,C*). These data suggest that the GIRK1 protein is expressed differentially in brain as follows: hippocampus ~ cortex ≫ thalamus ~ cerebellum ≫ medulla-pons. Preblocking the C-Ab prevented the immunoreactivity, which indicated that these are specific GIRK1 protein bands (data not shown). We have also noticed that the GIRK1 protein band from brain runs on PAGEs of different percentages with different degrees of dispersion, which may indicate different degrees of post-translational modifications, such as glycosylation, to the core polypeptide (calculated MW, 57.5 kDa).

Localization of GIRK1 protein in rat brain by immunocytochemistry

The overall pattern of immunostaining with anti-GIRK1 antibodies in the rat brain was similar to that observed by *in situ* hybridization (Fig. 4). There is prominent staining of the olfactory bulb, hippocampus, dentate gyrus, cerebellar cortex, thalamus, neocortex, and several nuclei in the brain stem and little to no staining in basal ganglia. For the most part, white matter displayed little staining. Parallel sections treated with sera preincubated with an excess of GIRK1 peptide displayed no signal above background (data not shown).

Expression of GIRK1 protein in somatic, dendritic, and axonal membranes in the hippocampal formation

Most neuronal populations expressing GIRK1 mRNA also express somatic and/or dendritic protein. In the hippocampal formation, GIRK1 mRNAs seemed to be expressed predominantly in pyramidal and granule cells. Strong *in situ* hybridization signals with GIRK1 probes were observed throughout the pyramidal cell layers of the hippocampus and the granule cell layer of the dentate gyrus (Fig. 5*A*). Signals seem stronger in the CA1 than in the CA3 fields. Weak to background hybridization signals are seen in all other hippocampal layers. Compared with hippocampal principal cells, interneurons here seem not to express GIRK1 transcripts.

In contrast, GIRK1 antibodies immunostained most layers of the hippocampus and area dentata (Fig. 5*B*). There was relatively weak immunostaining of pyramidal and granule cell somas (Fig. 5*C–E*). Stronger labeling, not associated with cell bodies, was seen in other layers (Fig. 5*B*). Strongest was the labeling of the stratum lacunosum moleculare of the hippocampus, followed by the immunostaining of the superficial (closer to the hippocampal fissure) half of the molecular layer of the dentate gyrus. Weaker but distinct labeling was also observed in the stratum oriens and the stratum radiatum, particularly the superficial half. The stratum lucidum in CA2 and CA3 and the polymorphic layer of the dentate gyrus showed weak to no staining. The pattern of immunostaining was identical in the septal and temporal portions of the hippocampal formation (data not shown).

Higher magnification of the stratum lacunosum moleculare shows that the strong staining here is associated with fibers that seem to cross the hippocampus along its long axis (Fig. 5*E,F*). Strong, labeled puncta suggestive of terminal labeling are also seen. Although a contribution of fibers of the perforant path cannot be discounted, we think that a more likely interpretation is that the staining is in the axons and terminals of the hippocampal projection of the nucleus reuniens of the midline thalamus (Wouterlood et al., 1990; Amaral and Witter, 1995). This interpretation is consistent with the observation described below that cortical projections of the thalamus are also immunostained. Moreover, the staining is significantly decreased after kainate lesioning of the thalamus (Fig. 8*F*).

GIRK1 protein in the apical and basal dendrites of CA1–CA3 pyramidal cells is probably the cause of most of the immunostaining seen in the stratum oriens and stratum radiatum (Fig. 5*B,E,F*). The orientation of the stained fibers in these areas is consistent with such interpretation. The staining in the molecular layer of the area dentata (Fig. 5*D*) could be attributable to immunostaining of the dendrites of granule cells, but a contribution from fibers from the lateral perforant path is also possible. The lack of staining on the stratum lucidum around the CA2–CA3 area (Fig. 5*B*) indicates that the mossy fiber containing the projections of the granule cells to the CA3 pyramidal cells is not labeled. Similarly, most interneurons in the hippocampus do not seem labeled, except for a few hilar cells (Fig. 5*D*).

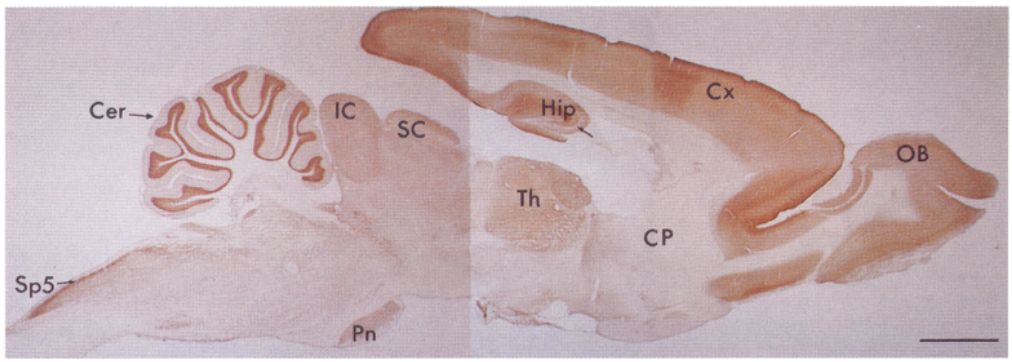

Figure 4. Immunolocalization of GIRK1 protein. Low-power bright-field photomicrograph of a sagittal section of a rat brain immunostained with the anti-GIRK1 antibodies. Note the strong immunostaining of the olfactory bulb, neocortex, hippocampus, and cerebellar cortex as well as the moderate staining of the thalamus, superior and inferior colliculi, pontine nucleus, and spinal trigeminal nucleus, and the weak signal in the caudate–putamen. *Cer*, Cerebellar cortex; *CP*, caudate–putamen; *Cx*, neocortex; *Hip*, hippocampal formation; *IC*, inferior colliculus; *OB*, olfactory bulb; *Pn*, pontine nucleus; *SC*, superior colliculus; *Sp5*, spinal trigeminal nucleus; *Th*, dorsal thalamus. Scale bar, 2.0 mm.

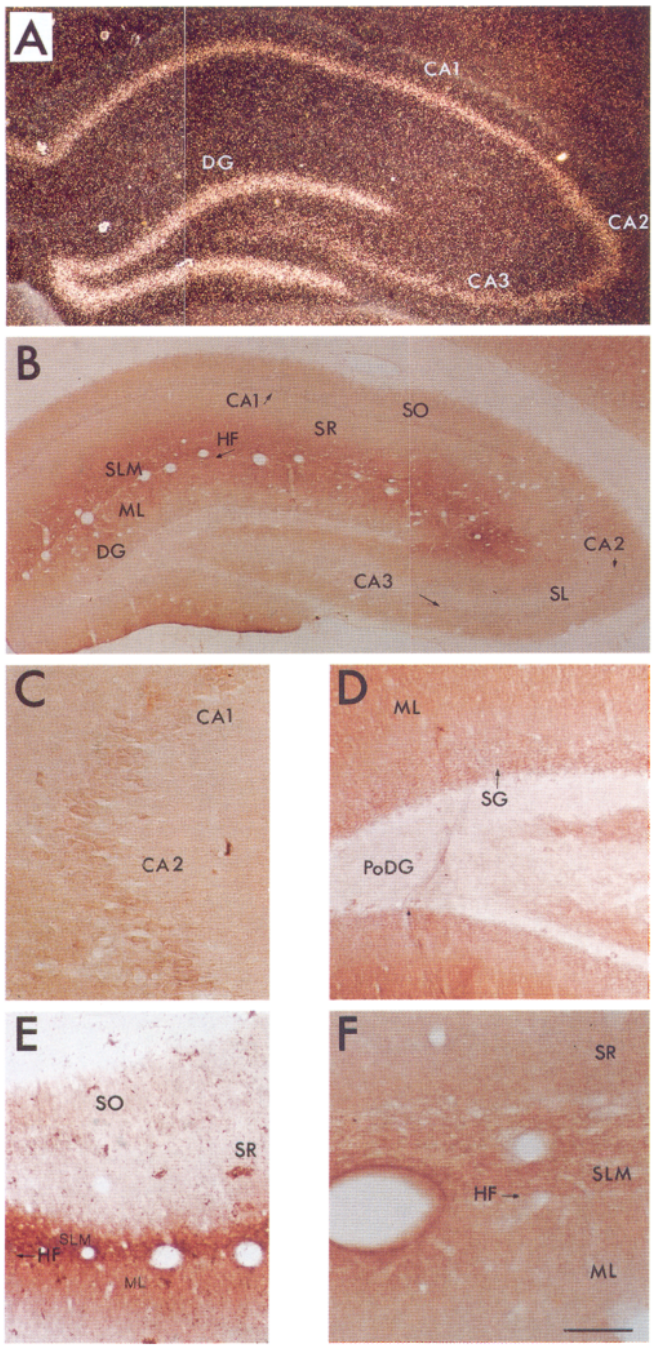

Figure 5. Localization of GIRK1 protein in the hippocampus. *A*, Dark-field photomicrograph of the hippocampal area after *in situ* hybridization histochemistry with the GIRK1-specific 5′ probe and counterstaining with cresyl violet. Note the strong hybridization signals in the pyramidal cell layers of the CA1–CA3 (*CA1, CA2, CA3*) fields of the hippocampus and in the granule cell layer of the dentate gyrus (*DG*). *B*, Bright-field photomicrograph of the hippocampal area after immunostaining with the anti-GIRK1 antibodies. Note that compared with background, as in the white matter surrounding the hippocampal formation, most of the hippocampal area is stained. The strongest staining is seen immediately above the hippocampal fissure (*HF*) in the stratum lacunosum moleculare (*SLM*) and the molecular layer of the area dentata (*ML*). The stratum lucidum (*SL*) and the dentate gyrus hilus have close to background staining. *C*, Higher-power image of the CA2 region of the section shown in *B*, illustrating the staining of pyramidal cell somata. *D*, High-power bright-field photomicrograph of the dentate gyrus after immunostaining with the anti-GIRK1 antibodies from another hippocampal section, illustrating the staining of granule cells in the stratum granulosum (*SG*). *E*, Medium-power bright-field photomicrograph around the CA1 portion of the hippocampus after immunostaining with a lower concentration of anti-GIRK1 antibodies (1:200 dilution) than in the sections shown in *B–D*, to illustrate that the staining of the stratum lacunosum moleculare and the molecular layer of the area dentata are significantly stronger than other parts of the hippocampal formation. Note the fiber-staining in the stratum oriens (*SO*) and in the *ML* and *SLM*. *F*, High-power bright-field photomicrograph of the section shown in *C*, illustrating the fiber-like pattern of staining in the stratum lacunosum moleculare. Other abbreviations: *DG*, dentate gyrus; *PoDG*, polymorphic layer of the dentate gyrus; *SR*, stratum radiatum. Scale bar: 450 μm in *A*; 390 μm in *B*; 50 μm in *C*; 100 μm in *D*; 200 μm in *E*; 80 μm in *F*.

Expression of GIRK1 protein in the cerebellar cortex

The cerebellar cortex is another area in which strong labeling was observed by *in situ* hybridization with GIRK1 cDNA probes. In this part of the brain, GIRK1 mRNAs are concentrated in the granule cell layer with little or no labeling elsewhere (Fig. 6*A*). Anti-GIRK1 antibodies also immunostained predominantly the granule cell layer (Fig. 6*B*). Little staining for mRNA or protein is seen in the molecular layer and in the white matter.

In the granule cell layer, granule cell somatic membrane is stained, albeit weakly, as compared with the staining of the glomeruli where granule cell dendrites synapse with mossy fiber terminals (Fig. 6*C,D*). In sections treated with osmium (Fig. 6*D*), it is possible to see clearly that the center of the glomeruli is unstained, indicating that the mossy fiber axons are not labeled. We conclude that in granule cells, GIRK1 protein is concentrated in the distal portion of granule cell dendrites. This interpretation was corroborated by electron microscopy immunohistochemistry (Fig. 7). Some dark immunoreaction product is seen on granule

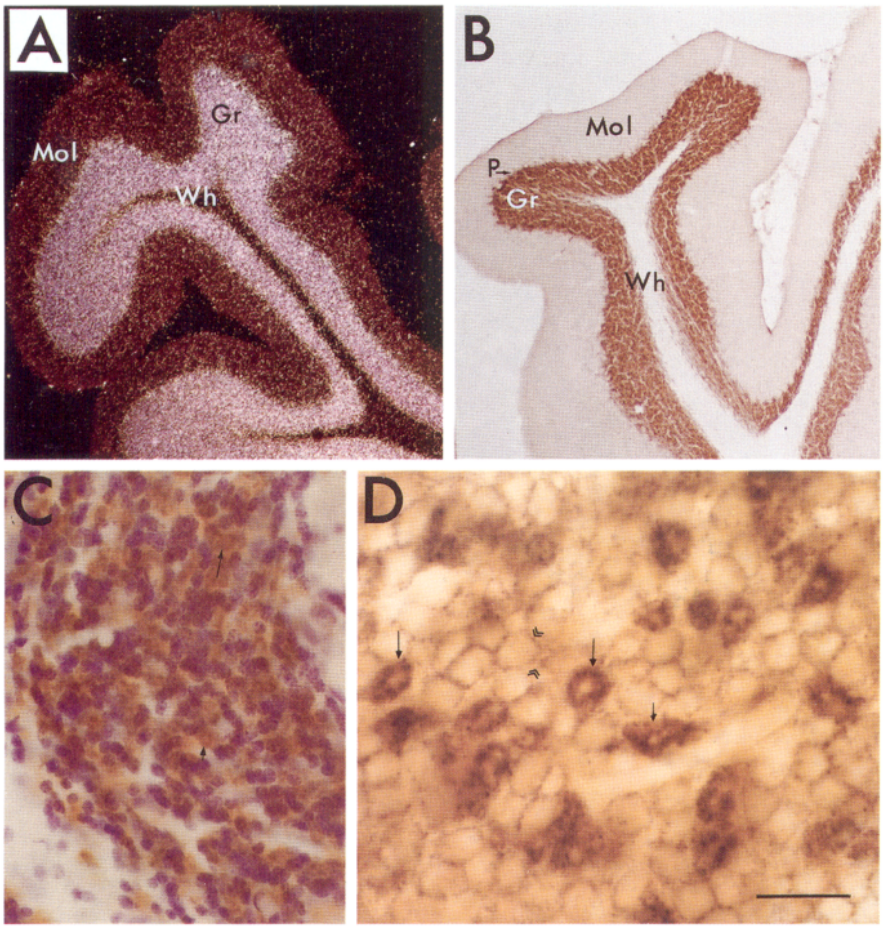

Figure 6. Localization of GIRK1 protein in the cerebellar cortex. *A*, Dark-field photomicrograph of the cerebellar cortex after *in situ* hybridization histochemistry with the GIRK1-specific cDNA 3′ probe and counterstaining with cresyl violet. Note strong hybridization signals in the granule cell layer (*Gr*). *B*, Low-power bright-field photomicrograph of the cerebellar cortex after immunostaining with the anti-GIRK1 antibodies. Note the strong staining of the granule cell layer and weak or no staining in Purkinje cells (*P*), molecular layer (*Mol*), and white matter (*Wh*). *C*, Medium-power image of the granule cell layer of the cerebellar cortex after immunostaining with the anti-GIRK1 antibodies and counterstaining with cresyl violet. Note that antibody-staining (*brown*) is seen predominantly in the glomeruli (*arrows*) and not in surrounding granule cell somas (*blue*). *D*, High-power image of the granule cell layer of the cerebellum after immunostaining with the anti-GIRK1 antibodies and postfixation with osmium (Weiser et al., 1995). Note the weak staining of the granule cell somata (*double arrowheads*) and the strong staining of the glomeruli (*arrows*). Also note that the center of the glomeruli, containing the mossy fiber axon, is not stained. Scale bar: 300 μm in *A*, *B*; 50 μm in *C*; 18 μm in *D*.

cell somata and proximal dendrites (data not shown), but stronger labeling is seen in distal dendrites in the area of the glomeruli around unstained mossy fiber terminals (Fig. 7). Generally, the label was concentrated in the vicinity of the plasma membrane and adjacent cytoplasm. In some dendrites, there is GIRK1 protein in the endoplasmic reticulum close to mitochondria (Fig. 7*A,C, left*). Immunoperoxidase precipitates were not seen in parallel sections treated without primary antibody or with antibody preincubated with excess peptide (data not shown).

GIRK1 protein in cortical dendrites and thalamocortical projections

Moderate *in situ* hybridization signals with GIRK1 cDNA probes were observed in the reticular thalamic nucleus and throughout most of the dorsal thalamus (Fig. 2*B–D*). Signals were stronger in the anterior thalamic nuclei than in more posterior nuclei, such as the medial geniculate (data not shown). The pattern of immunostaining was similar to that seen with *in situ* hybridization (Fig. 8*A*). Thalamic relay neuron somata are moderately stained (see *inset* in Fig. 8*A*). There is also staining of the neuropile throughout the thalamus.

Although pyramidal neurons in the neocortex express GIRK1 mRNAs, which are particularly strong in cells in layers II–III and V–VI (data not shown) (Karschin et al., 1994), there is only very faint immunostaining of neuronal cell bodies here, which usually is difficult to detect in experiments without nickel amplification (Fig. 8*B*); however, there is strong staining of neocortical fibers. Most prominent is the staining of fibers that run in a direction perpendicular to the surface of the cortex (Fig. 8*B,C*); particularly strong are fibers that run between layers I and III (Fig. 8*C*). These fibers are most likely the dendrites of pyramidal cells. In addition there is a diffuse, fiber-like band of immunostaining in layer IV of the cerebral cortex (indicated by *curved arrows* in Fig. 8*A*). This layer contains the terminals of thalamocortical projections, the axons of thalamic relay neurons (Jones and Burton, 1976; Herkenham, 1980; Jones, 1985; Steriade et al., 1990). Moreover, the band of immunostaining seen with anti-GIRK1 antibodies in layer IV of the cortex resembles the images in the parietal area observed when the thalamocortical terminals of somatosensory nuclei are revealed by a number of methods, such as the Fink-Heimer staining of degenerating thalamocortical terminals (Killackey, 1973). As in these cases, the band of immunostaining on layer IV is not homogeneous but consists of stained cylinders separated by less stained septa (Fig. 8*B,G*). These cylinders represent the cortical barrels (discrete multicellular units representing the cortical fields of somatosensory units) in cross-section.

To confirm that thalamocortical projections contribute to the immunostaining in the cortex, we examined the pattern of staining seen after unilateral kainate lesions of the thalamus. Kainic acid is an excitotoxic neurotoxin that specifically destroys cells (such as thalamic relay neurons) expressing cell-surface kainate receptors. Thus, when injected into the thalamus, thalamic relay neurons are destroyed, whereas afferent fibers, fibers of passage, and glial cells are spared (Coyle et al., 1978; Marty et al., 1991; Vukelic et al., 1991). In the experiment illustrated in Figure 8*D–H*, the brains were dissected out 6 d after the lesion and processed for histology and GIRK1 immunohistochemistry. The extent of the primary

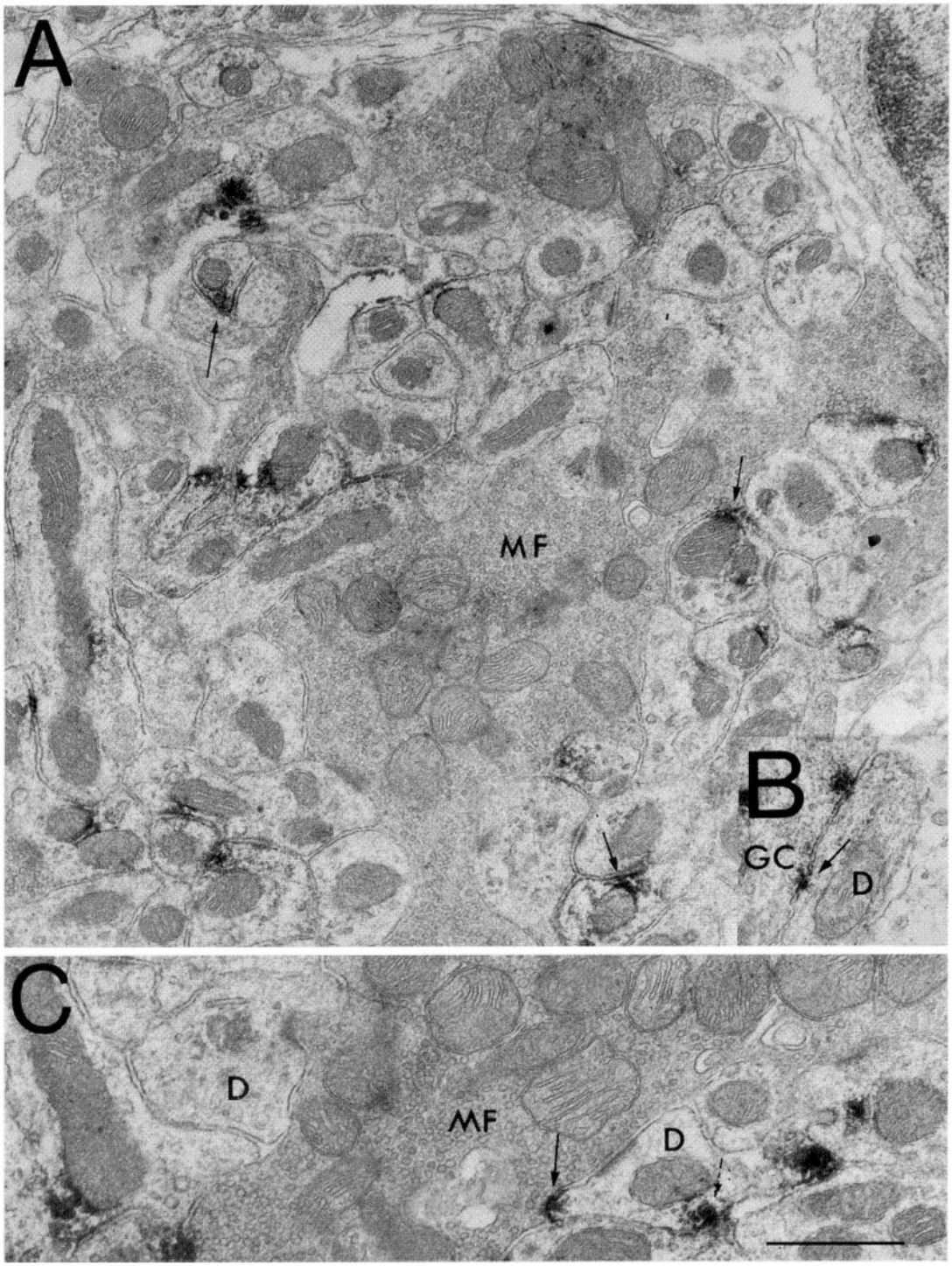

Figure 7. Electron microscopic immunolocalization of GIRK1 protein in the cerebellar cortex. *A*, Electron micrograph of a glomerulus in the granule cell layer of the cerebellar cortex, demonstrating deposition of immunoreaction product in the plasma membrane and in underlying cytoplasm of granule cell dendrites (*arrows*) surrounding the mossy fiber (*MF*). A portion of a granule cell is seen at the *top right*. *B*, Electron micrograph illustrating immunostaining in both the plasma membrane and the underlying cytoplasm of a granule cell (*GC*) and a dendrite (*D*) in contact with it. *C*, Higher-power electron micrograph of a glomerulus, illustrating staining in dendrites (*D*) surrounding a mossy fiber terminal (*MF*). Scale bar: 0.5 μm in *A*, *B*; 0.4 μm in *C*.

lesion in the thalamus is associated with a loss of staining (Fig. 8*E*). In this particular animal, the lesion extends to the midline. On the side ipsilateral to the lesion (*right side*), cortical layer IV shows a marked reduction in stain relative to that of the contralateral cortex, whereas the staining of dendrites and deep layers was largely unaffected by the lesion (Fig. 8*D,E,G,H*). This effect was specific to those cortical areas innervated by the lesioned thalamus. For example, the band of immmunostaining in layer IV was unaffected by the treatment in the temporal area of the cortex, consistent with the lack of lesioning in the medial geniculate body

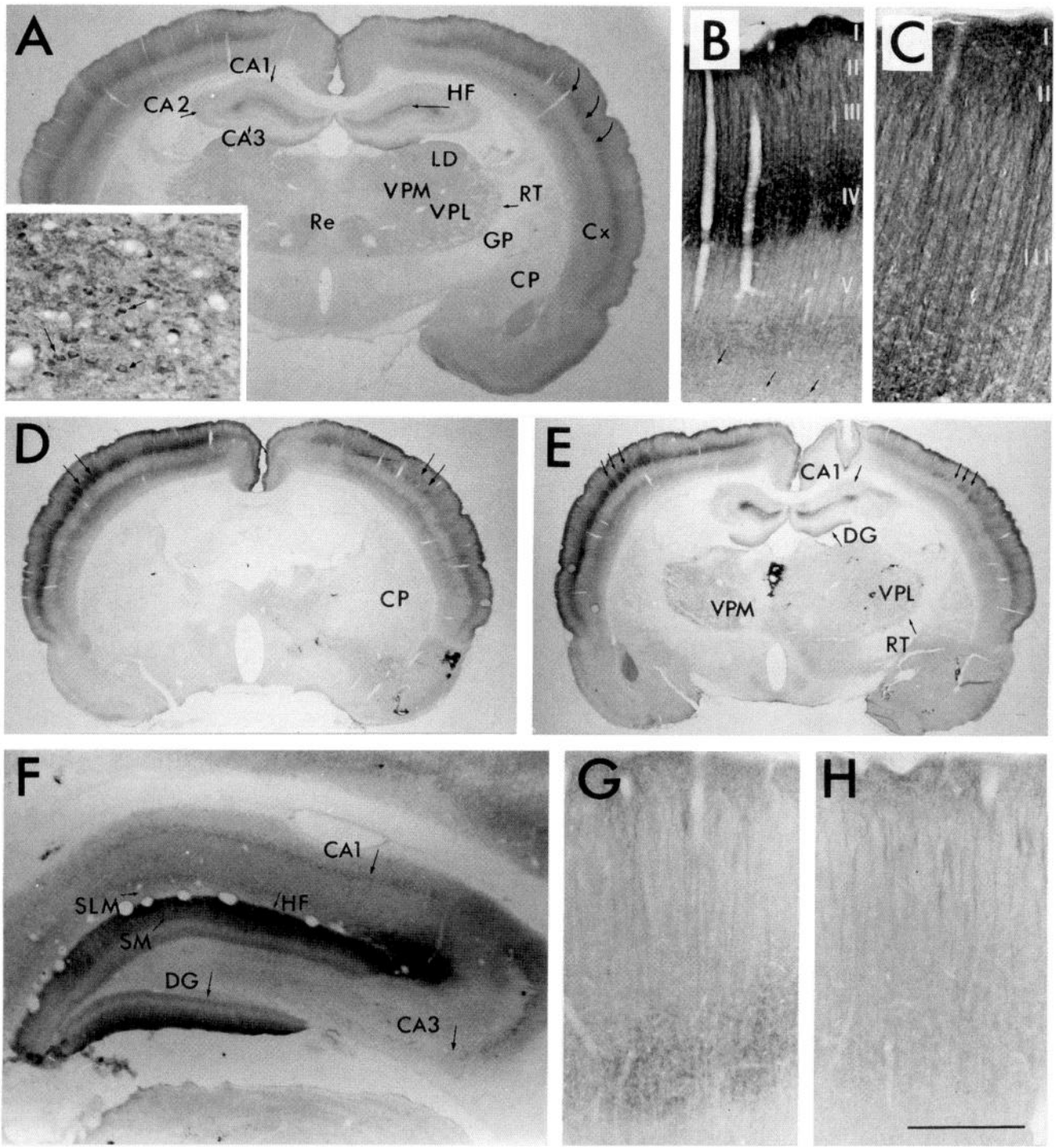

Figure 8. Localization of GIRK1 subunits in the neocortex and the thalamus. *A*, Low-power bright-field photomicrograph of a coronal section of rat brain immunostained with the anti-GIRK1 antibodies, illustrating the immunostaining of the cortex, the hippocampus, and the thalamus. The *insert* shows a high-power view of the ventroposteriomedial nucleus of the thalamus, illustrating the staining of the neuropile and of thalamic relay neuron somata. *B* and *C* show a higher magnification of the I–V and I–III layers of the cortex, respectively. Note the strong staining of pyramidal cell dendrites. Note in *B* (see also *G*) that at this magnification the band of immunostaining on layer IV is not homogeneous but consists of stained cylinders (representing the cortical barrels in cross-section) separated by less-stained septa. *D*, *E*, Immunohistochemistry with anti-GIRK1 antibodies of coronal sections from the brain of a rat injected unilaterally (on the *right side*) with kainic acid. The extent of the primary lesion in the ventral posterior thalamus (in the ventroposterolateral and ventroposteromedial nuclei, *VPL* and *VPM*) is associated with a loss of staining, as seen in *E*. The site of entrance of the injection needle on the *right* is also apparent in the section shown in *E*. Note that cortical layer IV on the side ipsilateral to the lesion shows a marked reduction in stain relative to that of the contralateral cortex, whereas the dendritic staining is largely unchanged (*arrows* point to cortical barrels). *F*, Bright-field micrograph of the right hippocampus of the lesioned rat shown in *D* and *E*. Note the reduced staining above the hippocampal fissure (*HF*). *G*, *H*, High-power micrographs of primary somatosensory cortex ipsilateral (*H*) and contralateral (*G*) to the lesioned side stained with anti-GIRK1 antibodies, showing the marked reduction of label in layer IV on the ipsilateral side. Other abbreviations: *CA1*, CA1 region of the hippocampus; *CA2*, CA2 region of the hippocampus; *CA3*, CA3 region of the hippocampus; *CP*, caudate–putamen; *Cx*, neocortex; *DG*, dentate gyrus; *GP*, globus pallidus; *LD*, laterodorsal thalamic nucleus; *Re*, reuniens thalamic nucleus; *RT*, reticular thalamic nucleus; *SLM*, stratum lacunosum moleculare; *SM*, stratum moleculare of the dentate gyrus. Scale bar: 2.6 mm in *A*; 300 μm for the *inset* in *A*; 0.5 mm in *B*; 0.2 mm in *C*; 3.4 mm in *D*, *E*; 0.74 mm in *F*; 0.3 mm in *G*, *H*.

(data not shown). These data provide compelling evidence for the presence of GIRK1 proteins in thalamocortical terminals. The lesion also produced a reduction in the immunostaining in the stratum lacunosum moleculare of the hippocampus (compare the staining above the hippocampal fissure in Fig. 8*F* with that in Figs. 5*B,E* and 8*A*). This result supports the view that the fibers stained here are also of thalamic origin.

GIRK1 protein in the cell bodies of neurons from brain stem nuclei

Neurons in deep cerebellar nuclei and several brainstem nuclei displayed clear somatodendritic staining (Fig. 9). We illustrate as examples the expression of somatic GIRK1 protein in neurons in the superior olive and the nucleus of the trapezoid body (Fig. 9*C*). The cell bodies and primary dendrites of neurons in the reticular formation are also strongly stained (Fig. 9*D,E*). In addition, there is profuse staining of fibers in the reticular core (Fig. 9*D,E*), which may represent fine dendrites of reticular neurons and/or axons of neurons projecting to the reticular formation.

The cell bodies of neurons in the central nucleus of the inferior colliculus are also stained clearly (Fig. 9*F*). Immunostaining of the neuropile is seen throughout the inferior colliculus; moreover, stained fibers are seen crossing on the commissure of the inferior colliculus (Fig. 9*F*).

The immunostaining of the neuropile with GIRK1 antibodies is extensive throughout the brain, and it is likely that much of this staining is in projecting fibers from GIRK1-expressing neurons. Given the extensive overlap of projections from GIRK1-expressing neuronal populations, however, it was not possible to ascertain the origin of the projections. Nevertheless, it is clear from the data illustrated here that not all projecting axons and terminal fields of GIRK1-expressing neurons are stained, as in the case of the axons of cerebellar granule cells (the parallel fiber system), the axons of the granule cells of the dentate gyrus (the hippocampal mossy fiber), and the axons of cells such as those in the pontine nucleus projecting to cerebellar granule cells (the cerebellar mossy fibers).

DISCUSSION

A number of GIRK channels have been cloned recently from rat atria and brain: GIRK1 or KGA1 (Dascal et al., 1993; Kubo et al., 1993) and GIRK2 and GIRK3 (Lesage et al., 1994). In the present study, we have localized the GIRK1 protein by immunohistochemical techniques to different regions of the rat brain, such as the olfactory bulb, hippocampus, dentate gyrus, cerebellar cortex, thalamus, neocortex, and several brain stem nuclei and have found little or no immunostaining in basal ganglia. Furthermore, the GIRK1 protein is present in different subcellular compartments, depending on the neuronal population. For example, the GIRK1 protein is predominantly dendritic in pyramidal cells of the neocortex and hippocampus as well as granule cells of the dentate gyrus and cerebellar cortex. In these neuronal populations, the staining of dendrites is much stronger than that of neuronal somas. By using immunohistochemistry with electron microscopy, we were able to show expression of GIRK1 protein in the postsynaptic membrane in dendritic buttons in the glomeruli in the granule cell layer of the cerebellar cortex. In the neuronal types with strong dendritic staining, GIRK channels are thus likely to influence postsynaptic integration of input signals mediated by neurotransmitters, which are released on synapses made predominantly on dendrites.

In other neuronal populations, however, notably in several nuclei of the brain stem, somatic immunostaining with anti-GIRK1 antibodies was very strong (Fig. 9). In these cells, GIRK channels may mediate the effects of synaptic transmission taking place at the soma. The localization of GIRK1 proteins in dendritic and somatic postsynaptic membrane is consistent with their role as components of ligand-gated channels. Because they are activated by G-protein subunits in a membrane-delimited fashion, one would expect the channels to be localized close to the neurotransmitter receptors to which they are functionally coupled.

More surprising was the finding of GIRK1 protein in axons and terminal fields. Strong evidence was provided for the presence of GIRK1 protein in thalamocortical terminals in cortical layer IV and in axons and terminals in the stratum lacunosum moleculare in the hippocampus. Although presynaptic neurotransmitter receptors exist and play a role in inhibiting neurotransmitter release and synaptic transmission (Chesselet, 1984; Cherubini and North, 1985; Hevron et al. 1986; North, 1986; Gray et al., 1989; Caudle and Chavkin, 1990; Pinnock, 1992; Vogt et al., 1992; Wagner et al., 1992; Chavez-Noriega and Stevens, 1994), to our knowledge this work provides the first evidence that GIRK channels may be the mediators of some of these effects. The inhibition of neurotransmitter release by activation of presynaptic receptors is probably the result of regulation of a number of processes in the nerve terminal, which could include modulation of ion channels such as those containing GIRK1 proteins. For example, evidence has been presented that a κ opioid receptor-agonist modulates ionic conductances in chick presynaptic calyciform nerve terminals with the predominate effect being hyperpolarization of the membrane, which would be expected to lead to inhibition of neurotransmitter release, apparently because of modulation of a K^+- and Na^+-dependent inward rectifier channel (Fletcher and Chiappinelli, 1992, 1993). To our knowledge, it is unknown whether this type of presynaptic K^+/Na^+ inward rectifier channel is present in mammalian nerve terminals and whether it is functionally similar to GIRK channels. Several receptors have been localized to thalamocortical terminals, most notably μ opiate receptors (Sahin et al., 1992; Vogt et al., 1992; Mansour et al., 1994, 1995), suggesting that GIRK channels may mediate the effects of these receptors. Moreover, μ opiate receptors activate GIRK1 channels expressed *in vitro* (Chen and Yu, 1994; Kovoor et al., 1995) and are also abundant in the stratum lacunosum moleculare of the hippocampus, probably in projections from the thalamic reuniens nuclei, because as observed here for GIRK1, there is no μ opiate receptor mRNA in this layer of the hippocampus but there is in the reuniens nucleus (Mansour et al., 1994, 1995).

The molecular mechanisms that result in distinct subcellular distributions of GIRK1 proteins in different neuronal populations remain to be elucidated. GIRK1 proteins might be associated with other subunits that could vary from one neuronal population to another and carry distinct membrane-sorting signals. In the case of $GABA_A$ receptors, the subcellular localization of the heteromeric channel can be dictated by one of the subunits (Perez-Velazquez and Angelides, 1993). The subunits that may associate with GIRK1 proteins to form heteromeric channels could be other proteins of the GIRK family, such as the recently cloned GIRK2 and GIRK3 cDNAs (Lesage et al., 1994) or perhaps even other inward rectifier proteins, which by themselves do not produce channels that are activated by G-proteins. For example, a protein related to GIRK1 in atria called CIR or KATP (Ashford et al., 1994; Krapivinsky et al., 1995), which by itself does not express G-protein-activated channels, seems to form heteromultimers with GIRK1 and to potentiate the expression of GIRK channels (Krapivinsky et al., 1995). The GIRK1

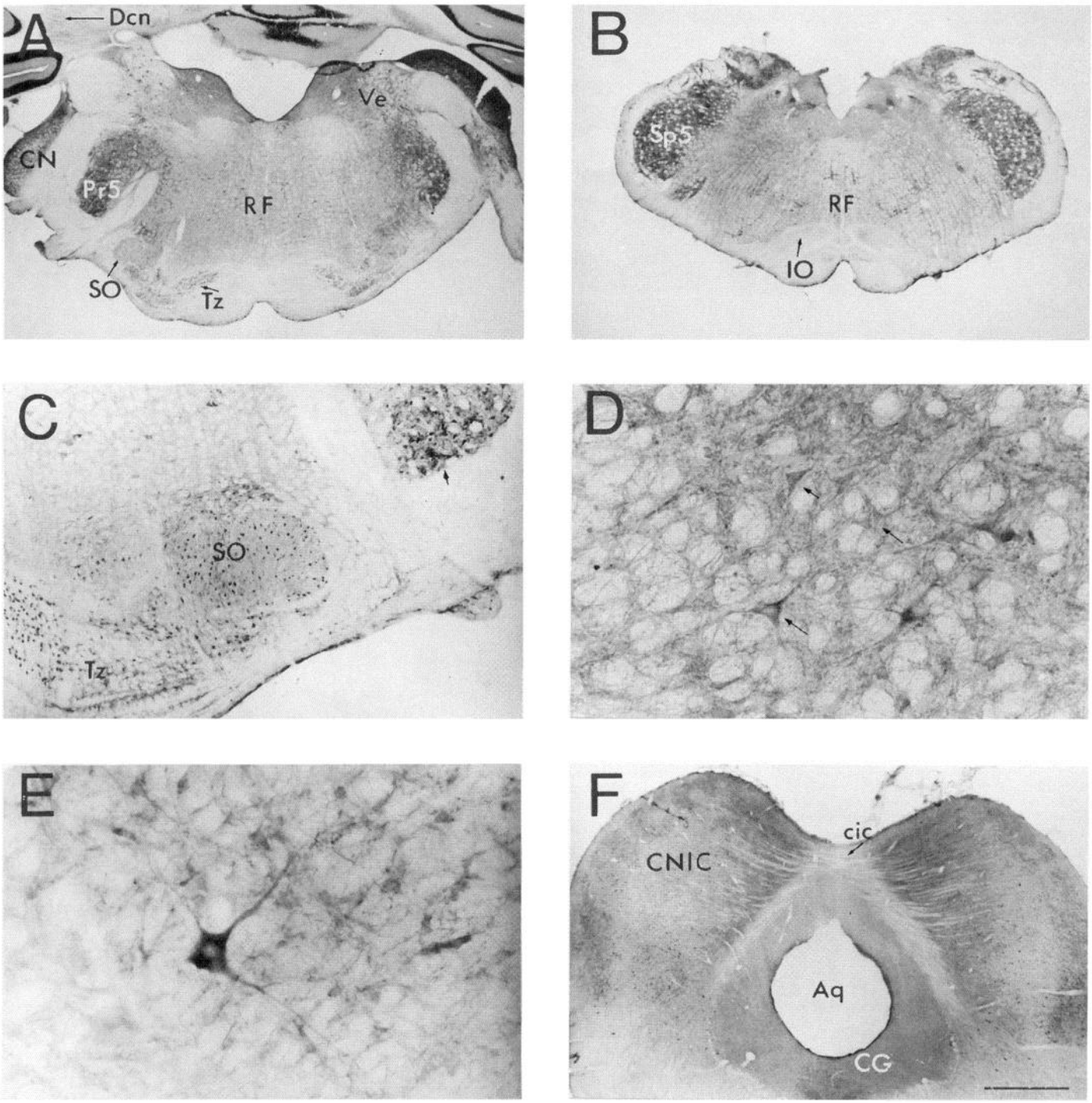

Figure 9. Localization of GIRK1 proteins in brain stem neurons. *A*, *B*, Low-power bright-field photomicrographs of the medulla after immunostaining with anti-GIRK1 antibodies. Note the staining throughout the reticular formation (*RF*) and the labeling of deep cerebellar nuclei (*Dcn*), cochlear nuclei (*CN*), the principal sensory and spinal nuclei of the trigeminal nerve (*Pr5* and *Sp5*, respectively), vestibular nuclei (*Ve*), superior olive (*SO*), and nucleus of the trapezoid body (*Tz*). The inferior olive (*IO*) is only very weakly stained. *C*, Medium-power bright-field photomicrograph of the ventral portion of the section shown in *A*, illustrating the staining of neurons in the superior olive and the nuclei of the trapezoid body and the trigeminal nerve (*arrow*). *D*, *E*, Medium- and high-power images, respectively, of the reticular formation, illustrating strong somatodendritic staining (*arrows* in *D*) as well as staining of the reticular net. *F*, Bright-field photomicrograph of a coronal section at the level of the inferior colliculus after immunostaining with the anti-GIRK1 antibodies. Other abbreviations: *Aq*, aqueduct; *CG*, central gray; *CNIC*, central nucleus of the inferior colliculus; *cic*, commissure of the inferior colliculus. Scale bar: 1.4 mm in *A*; 1.2 mm in *B*; 300 μm in *C*; 120 μm in *D*; 60 μm in *E*; 0.93 mm in *F*.

protein may also anchor to intracellular proteins that vary from one neuronal population to another. Differential extracellular interactions or post-translational processing also may result in varying localizations (Nelson et al., 1992; Rodriguez-Boulan and Powell, 1992; Kelly and Grote, 1993; Pelham and Munro, 1993; Craig and Banker, 1994).

The predominantly dendritic pattern of expression of GIRK1 proteins in some neuronal populations is similar to that observed for

Kv4.2 proteins. Like GIRK1, Kv4.2 proteins, which are components of A-type voltage-gated K^+ channels, prevail in dendrites rather than somas in granule cells in the cerebellum and in pyramidal cells in the neocortex and hippocampus and are present throughout the dendritic tree, including fine dendritic processes (Sheng et al., 1992) (E. Bueno, A. Chow, and B. Rudy, unpublished observations). The specificity of this pattern of expression can be illustrated by comparing the localization of GIRK1 and Kv4.2 proteins with the localization of Kv3.1b proteins, also components of voltage-gated channels, in cerebellar granule cells (Weiser et al., 1995). Unlike the antibodies against Kv4.2 and GIRK1, which immunostain predominantly the glomeruli, with Kv3.1b antibodies, granule cell somata are strongly stained but the glomeruli show only faint staining [compare Fig. 7*C* of Weiser et al. (1995) with Fig. 6*G–J* of Sheng et al. (1992) and our Fig. 6*C,D*]. The data for these three proteins, in the same neuronal population, demonstrate that the "somatodendritic" membrane often treated as a single sorting compartment of the membrane is not homogeneous (Dotti and Simons, 1990; Rodriguez-Boulan and Powell, 1992; de Hoop and Dotti, 1993).

REFERENCES

Amaral DG, Witter MP (1995) Hippocampal formation. In: The rat nervous system, 2nd Ed (Paxinos G, ed), pp 443–493. Los Angeles: Academic.

Ashford MLJ, Bond CT, Blari TA, Adelman JP (1994) Cloning and functional expression of a rat heart KATP channel. Nature 370:456–459.

Ausubel FM, Brent R, Kingston RE, More DD, Seidman JG, Smith JA, Struhl (1990) Current protocols in molecular biology, Vol 1 and 2. New York: Wiley.

Breitwieser GE, Szabo G (1985) Uncoupling of cardiac muscarinic and β adrenergic receptors from ion channels by a guanine nucleotide analogue. Nature 317:538–540.

Brown AM, Birnbaumer L (1990) Ionic channels and their regulation by G protein subunits. Annu Rev Physiol 52:197–213.

Caudle R, Chavkin C (1990) μ opioid receptor activation reduces inhibitory postsynaptic potentials in hippocampal CA3 pyramidal cells of rat and guinea pig. J Pharmacol Exp Ther 252:1361–1369.

Chavez-Noriega LE, Stevens CF (1994) Increased transmitter release at excitatory synapses produced by direct activation of adenylate cyclase in rat hippocampal slices. J Neurosci 14:310–317.

Chen Y, Yu L, (1994) Differential regulation by cAMP-dependent protein kinase and protein kinase C of the μ opiate receptor coupling to a G protein-activated K^+ channel. J Biol Chem 269:7839–7842.

Cherubini E, North RA (1985) μ and κ opioids inhibit transmitter release by different mechanisms. Proc Natl Acad Sci USA 82:1860–1863.

Chesselet MF (1984) Presynaptic regulation of neurotransmitter release in the brain: facts and hypothesis. Neuroscience 12:347–375.

Codina J, Yatani A, Grenet D, Brown AM, Birnbaumer L (1987) The alpha subunit of GK opens atrial K channels. Science 236:442–445.

Coyle JT, Molliver ME, Kuhar MJ (1978) *In situ* injection of kainic acid: a new method for selectively lesioning neural cell bodies while sparing axons of passage. J Comp Neurol 180:301–324.

Craig AM, Banker G (1994) Neuronal polarity. Annu Rev Neurosci 17:267–310.

Dascal N, Schreibmayer W, Lim NF, Wang W, Chakin C, Dimagno L, Labarca C, Kieffer BL, Caveriaux-Ruff C, Trollinger D, Lester HA, Davidson N (1993) Atrial G protein-activated K^+ channel: expression cloning and molecular properties. Proc Natl Acad Sci USA 90:10235–10239.

de Hoop MJ, Dotti CG (1993) Membrane traffic in polarized neurons in culture. Epithelial and neuronal cell polarity and differentiation. J Cell Sci [Suppl] 17:85–92.

Dotti CG, Simons K (1990) Polarized sorting of viral glycoproteins to the axon and dendrites of hippocampal neurons in culture. Cell 62:63–72.

Fletcher GH, Chiappinelli VA (1992) An inward rectifier is present in presynaptic nerve terminals in the chick ciliary ganglion. Brain Res 575:103–112.

Fletcher GH, Chiappinelli VA (1993) The action of the κ opioid agonist U-50,488 on presynaptic nerve terminals of the chick ciliary ganglion. Neuroscience 53:239–250.

Gray DB, Pilar GR, Ford MJ (1989) Opiate and peptide inhibition of transmitter release in parasympathetic nerve terminals. J Neurosci 9:1683–1692.

Harlow E, Lane D (1988) Antibodies: a laboratory manual. Cold Spring Harbor, NY: Cold Spring Harbor Laboratories.

Hartshorne RP, Catterall WA (1984) The sodium channel from rat brain: purification and subunit composition. J Biol Chem 259:1667–1675.

Herkenham M (1980) Laminar organization of thalamic projections to the rat neocortex. Science 207:532–534.

Hevron E, David G, Arnon A, Yaori Y (1986) Acetylcholine modulates two types of presynaptic potassium channels in vertebrate motor nerve terminals. Neurosci Lett 72:87–92.

Hille B (1992) Ionic channels of excitable membranes, 2nd ed. Sunderland, MA: Sinauer.

Jones EG (1985) The thalamus. New York: Plenum.

Jones EG, Burton H (1976) Areal differences in the laminar distribution of thalamic afferents in cortical fields of the insular, parietal and temporal regions of primates. J Comp Neurol 168:197–248.

Karschin C, Schreibmayer W, Dascal N, Lester H, Davidson N, Karschin A (1994) Distribution and localization of a G protein-coupled inwardly rectifying K channel in the rat. FEBS Lett 348:139–144.

Kelly RB, Grote E (1993) Protein targeting in the neuron. Annu Rev Neurosci 16:95–127.

Killackey HP (1973) Anatomical evidence for cortical subdivision based on vertically discrete thalamic projections from the ventral posterior nucleus to cortical barrels in the rat. Brain Res 51:326–331.

Kovoor A, Henry DJ, Chavkin C (1995) Agonist-induced desensitization of the μ opioid receptor-coupled potassium channel (GIRK1). J Biol Chem 270:589–595.

Krapivinsky G, Gordon E, Wickman K, Velimirovic B, Krapivinsky L, Clapham DE (1995) The G-protein-gated atrial K channel I_{KAch} is a heteromultimer of two inwardly rectifying K-channel proteins. Nature 374:135–141.

Kubo Y, Reuveny E, Slesinger PA, Jan YN, Jan LY (1993) Primary structure and functional expression of a rat G-protein-coupled muscarinic K channel. Nature 364:802–806.

Lesage F, Duprat F, Fink M, Guillemare E, Coppola T, Lazdunski M, Hugnot JP (1994) Cloning provides evidence for a family of inward rectifier and G protein coupled K channels in the brain. FEBS Lett 353:37–42.

Logothetis DE, Kurachi Y, Galper J, Neer EJ, Clapman DE (1987) The beta-gamma subunits of GTP-binding proteins activate the muscarinic K channel in heart. Nature 325:321–326.

Mansour A, Fox CA, Thompson RC, Akil H, Watson SJ (1994) μ-opioid receptor mRNA expression in the rat CNS: comparison to μ-receptor binding. Brain Res 643:245–265.

Mansour A, Fox CA, Akil H, Watson SJ (1995) Opioid receptor mRNA expression in the rat CNS: anatomical and functional implications. Trends Neurosci 18:22–29.

Marty S, Dusart I, Peschanski M (1991) Glial changes following an excitotoxic lesion in the CNS: I. microglia/macrophages. Neuroscience 45:529–530.

Moreno H, Kentros C, Bueno E, Weiser M, Hernandez A, Vega-Saenz de Miera E, Thornhill W, Rudy B (1995) Thalamocortical projections have a K^+ channel that is phosphorylated and modulated by cAMP-dependent protein kinase. J Neurosci 15:5486–5501.

Nelson WJ (1992) Regulation of cell surface polarity from bacteria to mammals. Science 258:948–955.

North RA (1986) Opioid receptor types and membrane ion channels. Trends Neurosci 9:114–117.

North RA (1989) Drug receptors and the inhibition of nerve cells. Br J Pharmacol 98:13–28.

Paxinos G, Watson C (1986) The rat brain in stereotaxic coordinates, 2nd ed. Boca Raton, FL: Academic.

Pelham HR, Munro S (1993) Sorting of membrane proteins in the secretory pathway. Cell 75:603–605.

Perez-Velazquez JL, Angelides K (1993) Assembly of GABA-A receptor subunits determines sorting and localization in polarized cells. Nature 361:457–460.

Pfaffinger PJ, Martin JM, Hunter DD, Nathanson NM, Hille B (1985) GTP-binding proteins couple cardiac muscarinic receptors to a K channel. Nature 317:536–538.

Pinnock RD (1992) A highly sensitive K-opioid receptor agonist, CI-977, reduces excitatory synaptic potentials in the rat locus coeruleus in vitro. Neurosci Lett 78:22–28.

Reuveny E, Slesinger PA, Inglese J, Morales JM, Iniguez-Lluhi JA, Lefkowitz RJ, Bourne HR, Jan YN, Jan LY (1994) Activation of the cloned muscarinic potassium channel by G protein beta gamma subunits. Nature 370:143–146.

Rodriguez-Boulan E, Powell SK (1992) Polarity of epithelial and neuronal cells. Annu Rev Cell Biol 8:395–427.

Rudy B, Kentros C, Weiser M, Fruhling D, Serodio P, Vega-Saenz de Miera E, Ellisman MH, Pollock JA, Baker H (1992) Region-specific expression of a K^+ channel gene in brain. Proc Natl Acad Sci USA 89:4603–4607.

Sahin M, Bowen WD, Donoghue JP (1992) Location of nicotinic and muscarinic cholinergic and μ-opiate receptors in rat cerebral neocortex: evidence from thalamic and cortical lesions. Brain Res 579:135–147.

Sheng M, Tsaur M-L, Jan YN, Jan LY (1992) Subcellular segregation of two A-type K^+ channel proteins in rat central neurons. Neuron 9:271–284.

Steriade M, Jones EG, Llinas RR (1990) Thalamic oscillations and signaling. New York: Wiley.

Vogt BA, Crino PB, Jensen EL (1992) Multiple heteroreceptors on limbic thalamic axons: M_2 acetylcholine, serotonin$_{1B}$, b_2-adrenoceptors, [μ]-opioid, and neurotensin. Synapse 10:44–53.

Vukelic JI, Yamamoto T, Hertzberg EL, Nagy JI (1991) Depletion of connexin 43-immunoreactivity in astrocytes after kainic acid-induced lesions in rat brain. Neurosci Lett 130:120–124.

Wagner JJ, Caudle RM, Chavkin C (1992) κ-opioids increase excitatory transmission in the dentate gyrus of the guinea pig hippocampus. J Neurosci 12:132–141.

Weiser M, Vega-Saenz de Miera E, Kentros C, Moreno H, Franzen L, Hillman D, Baker H, Rudy B (1994) Differential expression of Shaw-related K^+ channels in the rat central nervous system. J Neurosci 14:949–972.

Weiser M, Bueno E, Sekirnjak C, Martone ME, Baker H, Hillman D, Thornhill W, Ellisman M, Rudy B (1995) The potassium channel subunit KV3.1b is localized to somatic and axonal membranes of specific populations of CNS neurons. J Neurosci 15:4298–4314 .

Wickman KD, Iniquez-Lluhi JA, Cavenport PA, Taussig R, Krapivinsky GB, Linder ME, Gilman AG, Clapham DE (1994) Recombinant G-protein beta/gamma subunits activate the muscarinic-gated atrial potassium channel. Nature 368:255–257.

Wouterlood FG, Saldana E, Witter MP (1990) Projection from the nucleus reuniens thalami to the hippocampal region: light and electron microscopic tracing study in the rat with the anterograde tracer Phaseolus vulgaris-leucoagglutinin. J Comp Neurol 296:179–203.

Yatani A, Mattera R, Codina J, Graf R, Okabe K, Padrell E, Iyengar R, Brown AM, Birnbaumer L (1988) The G-protein gated atrial K channel is stimulated by three distinct Gi alpha subunits. Nature 336:680–682.